

**Science**

 AAAS

**Thermodynamics and Kinetics of a Brownian Motor**

R. Dean Astumian, *et al.*

*Science* **276**, 917 (1997);

DOI: 10.1126/science.276.5314.917

***The following resources related to this article are available online at  
www.sciencemag.org (this information is current as of February 13, 2008 ):***

**Updated information and services**, including high-resolution figures, can be found in the online version of this article at:

<http://www.sciencemag.org/cgi/content/full/276/5314/917>

This article has been **cited by** 34 articles hosted by HighWire Press; see:

<http://www.sciencemag.org/cgi/content/full/276/5314/917#otherarticles>

This article appears in the following **subject collections**:

Chemistry

<http://www.sciencemag.org/cgi/collection/chemistry>

Information about obtaining **reprints** of this article or about obtaining **permission to reproduce this article** in whole or in part can be found at:

<http://www.sciencemag.org/about/permissions.dtl>

# Thermodynamics and Kinetics of a Brownian Motor

R. Dean Astumian

Nonequilibrium fluctuations, whether generated externally or by a chemical reaction far from equilibrium, can bias the Brownian motion of a particle in an anisotropic medium without thermal gradients, a net force such as gravity, or a macroscopic electric field. Fluctuation-driven transport is one mechanism by which chemical energy can directly drive the motion of particles and macromolecules and may find application in a wide variety of fields, including particle separation and the design of molecular motors and pumps.

A small particle in a liquid is subject to random collisions with solvent molecules. The resulting erratic movement, or Brownian motion, has been described theoretically by Einstein (1) and independently by Langevin (2). Langevin hypothesized that the forces on the particle due to the solvent can be split into two components: (i) a fluctuating force that changes direction and magnitude frequently compared to any other time scale of the system and averages to zero over time, and (ii) a viscous drag force that always slows the motions induced by the fluctuation term. These two forces are not independent: The amplitude of the fluctuating force is governed by the viscosity of the solution and by temperature, so the fluctuation is often termed thermal noise.

At equilibrium, the effect of thermal noise is symmetric, even in an anisotropic medium. The second law of thermodynamics requires this: Structural features alone, no matter how cleverly designed, cannot bias Brownian motion (3, 4). To illustrate this point, Feynman discussed the possibility of using thermal noise in conjunction with anisotropy to drive a motor in the context of a "ratchet and pawl" device shrunk to microscopic size (4). He showed that when all components of such a device are treated consistently, net motion is not achieved in an isothermal system, despite the anisotropy of the ratchet's teeth. However, a thermal gradient in synergy with Brownian motion can cause directed motion of a ratchet and can be used to do work. As a practical matter, large thermal gradients are essentially impossible to maintain over small distances. Particularly in biology and chemistry, the thermal gradients necessary to drive significant motion are not realistic.

It might seem then that, despite its per-

vasive nature, Brownian motion cannot be used to any advantage in separating or moving particles, either in natural systems (such as biological ion pumps and biomolecular motors) or by artificial devices. Recent work has focused, however, on the possibility of an energy source other than a thermal gradient to power a microscopic motor. If energy is supplied by external fluctuations (5–8) or a nonequilibrium chemical reaction (9, 10), Brownian motion can be biased if the medium is anisotropic, even in an isothermal system. Thus, directed motion is possible without gravitational force, macroscopic electric fields, or long-range spatial gradients of chemicals.

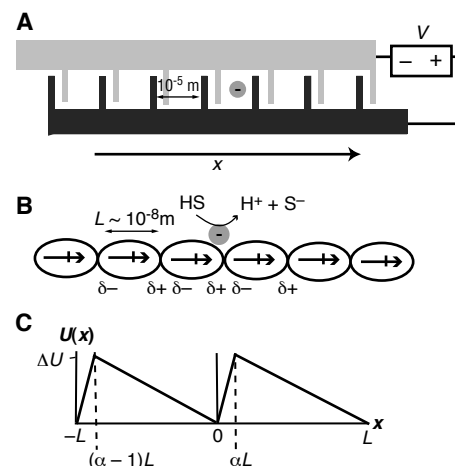
In devices based on biased Brownian motion, net transport occurs by a combination of diffusion and deterministic motion induced by externally applied time-dependent electric fields. Because particles of different sizes experience different levels of friction and Brownian motion, an

appropriately designed external modulation can be exploited to cause particles of slightly different sizes to move in opposite directions (11–16). One can imagine an apparatus where a mixture is fed into the system from the middle and purified fractions are continuously removed from either side. Because part of the energy required for transport over energy barriers is provided by thermal noise and because the external forces are exerted on a small length scale, such devices may be able to operate with small external voltages. In contrast, many conventional techniques, such as electrophoresis, centrifugation, and chromatography, must be turned off and on each time a new batch of particles is added. These methods rely on motion caused by long-range gradients, where the major influence of thermal noise is to degrade the quality of separation by diffusive broadening of the bands.

## Biased Brownian Motion

As a specific example of biased Brownian motion (Fig. 1A), picture a charged particle moving over an array of interdigitated electrodes with a spatial period of 10  $\mu\text{m}$ . When a voltage is applied, the potential energy of the particle is approximately an anisotropic sawtooth function (Fig. 1C). Although the electric generator is certain-

**Fig. 1.** Two specific models by which an anisotropic periodic potential can arise. **(A)** When a voltage difference  $V$  is applied to interdigitated electrodes deposited on a glass slide with anisotropically positioned "teeth," the resulting potential is spatially periodic but anisotropic. With photolithography it is possible to achieve a spatial period  $L$  for such a structure as small as  $10^{-5}$  m or even somewhat less. **(B)** A linear array of dipoles aligned head to tail on which a charged Brownian particle (possibly a protein) moves. The individual dipoles could be macromolecular monomers that aggregate to form an extended linear polymer. The length of the individual monomer is  $L \sim 10^{-8}$  m, a reasonable value for many aggregating proteins. If the particle catalyzes the reaction  $\text{HS} \rightarrow \text{H}^+ + \text{S}^-$ , the charge on the particle, and hence its electrostatic potential energy of interaction with the dipole array  $U(x, t)$ , fluctuates depending on its chemical state. **(C)** The potential  $U(x)$  for both (A) and (B) is approximately an anisotropic sawtooth function  $U_{\text{saw}}$ , drawn for simplicity as a piece-wise linear function. The amplitude is  $\Delta U$ , and the wells (potential minima) are spaced periodically at positions  $iL$ . The anisotropy is parameterized by  $\alpha$ . The amplitude  $\Delta U$  of the sawtooth potential can be modulated in (A) by using an external switching device to control the applied voltage.



The author is in the Departments of Surgery and of Biochemistry and Molecular Biology, University of Chicago, MC6035, Chicago, IL 60637, USA. E-mail: dastumia@surgery.bsdc.uchicago.edu

ly a macroscopic device, the electric field in the  $x$  direction averaged over a spatial period is zero no matter what the voltage, and so there is no net macroscopic force. A nonequilibrium fluctuation can be produced by using a switching device that imposes an externally defined but possibly random modulation of the voltage. Recent experiments have shown that unidirectional motion of microscopic particles can be induced by modulating the amplitude of such an anisotropic sawtooth potential (17, 18). Theory shows that the direction of flow is governed by a combination of the local spatial anisotropy of the applied potential, the diffusion coefficient of the particle, and the specific details of how the external modulation is carried out (11–16). Under some conditions, particles of slightly different sizes can move in opposite directions, possibly providing the basis for a continuous separation process. Several technological hurdles remain, however, before a practical device can be constructed.

In a second example (Fig. 1B), a

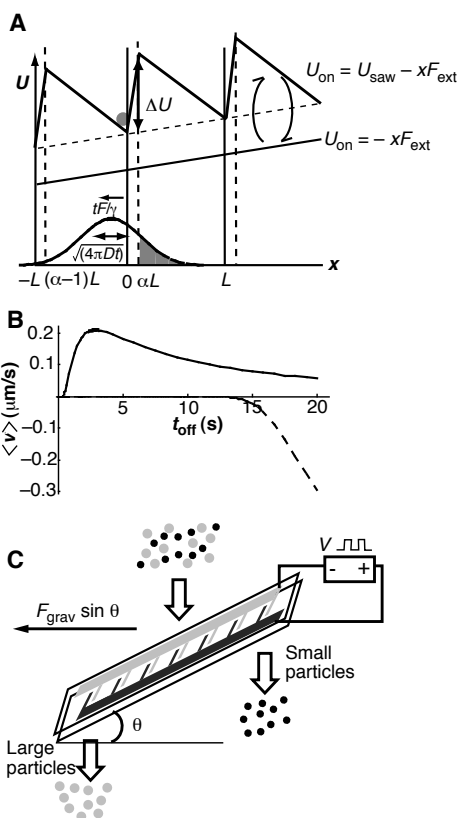
Brownian particle moves along a lattice of electric dipoles arranged head to tail (7). The individual dipoles could be, for example, macromolecular monomers that aggregate to form an extended linear polymer. Imagine that the particle has an active site to catalyze a hydrolysis reaction  $HS \rightarrow H^+ + S^-$ , where  $S$  denotes some substrate molecule. The charge on an individual particle will then fluctuate, depending on whether  $H^+$  or  $S^-$  is bound. The potential energy of the particle along the axis of the dipole lattice is approximately described by a sawtooth function (Fig. 1C), but the amplitude depends on the charge and hence on the chemical state. When the chemical reaction  $HS \rightarrow H^+ + S^-$  is far from equilibrium, the fluctuation of the charge on the particle due to the reaction can cause unidirectional transport. This effect may be important in the chemomechanical energy conversion of biomolecular motors and pumps, proteins that convert energy from a chemical reaction such as adenosine triphosphate (ATP) hydrolysis to drive

unidirectional transport. Although it is unlikely that any biological motor operates exactly as a simple Brownian ratchet using chemical energy to bias thermal noise, some of the basic principles of operation may be the same.

Recent experiments have shown that, consistent with a ratchet mechanism (5, 19, 20), external oscillating (21) or fluctuating (22) electric fields can drive transport by a molecular ion pump, the sodium-potassium adenosine triphosphatase. Energy from the field substitutes for the energy normally provided by ATP hydrolysis even though the average value of the field is zero. Fluctuation-driven transport provides an explicit mechanism for coupling energy from a nonequilibrium chemical reaction to cause local fluctuations similar to those imposed externally to drive unidirectional transport (20). Ultimately, it may be possible to construct microscopic motors and pumps that use nonequilibrium chemical reactions as their fuel.

The examples in Fig. 1 are provided to make our discussion more concrete. The general idea of diffusion on a periodic potential arises in many other contexts (23), including enzyme catalysis, where an enzyme cycles through several intermediate states in carrying out its function (19); the solid-state physics of transistors (24), where an electron moves through several  $p$ - $n$  junctions; models of Josephson junctions (25); and generalized models of computation (26). The details of the interactions giving rise to the potential are not as critical as the mechanisms by which spatial anisotropy conspires with thermal noise to allow energy from external fluctuations or a nonequilibrium chemical reaction to drive unidirectional flow. Anisotropic potentials such as that shown in Fig. 1C are known as ratchet potentials, in analogy to macroscopic ratchets such as a car jack that allow motion in only one direction by a series of asymmetric gears.

**Fig. 2.** How a fluctuating potential causes uphill transport. **(A)** Schematic representation of a fluctuating potential energy profile. When the potential is on, the potential energy  $U_{\text{on}}$  of a particle is a sawtooth function  $U_{\text{saw}} - xF_{\text{ext}}$  with periodically spaced wells at positions  $iL$ . The anisotropy of  $U_{\text{saw}}$  results in two legs of the potential, one of length  $\alpha L$  on which the force is  $-\Delta U/(\alpha L) + F_{\text{ext}}$ , and the other of length  $(1 - \alpha)L$  on which the force is  $\Delta U/[(1 - \alpha)L] + F_{\text{ext}}$ . When the potential is off, the energy profile is flat with force  $F_{\text{ext}}$  everywhere. The curve below the two potential profiles shows a Gaussian probability function resulting from turning the potential off at  $t = 0$ , with the particle starting at  $x = 0$ . The result is resolved into two components: the downhill drift and the diffusive spreading of the probability distribution. For intermediate times, it is more likely for a particle to be between  $\alpha L$  and  $(1 + \alpha)L$ , where it would be trapped in the well at  $L$  if the potential were turned back on, than between  $(\alpha - 1)L$  and  $(\alpha - 2)L$ , where it would be trapped in the well at  $-L$  if the potential were turned back on. Thus, turning the potential on and off cyclically can cause motion to the right despite the net force to the left. **(B)** Average velocity of a spherical particle with radius  $r_p = 2 \mu\text{m}$  (solid line) and  $r_p = 5 \mu\text{m}$  (dashed line) induced by cyclically turning an anisotropic sawtooth potential ( $\alpha = 0.1$ ) on and off versus the time spent in the off state  $t_{\text{off}}$  (with  $t_{\text{on}} = t_{\text{off}}$ ). The period was  $L = 10 \mu\text{m}$  with an external force due to gravity  $F_{\text{ext}} = V_p(d_p - d_w)g \sin(\theta)$ ;  $V_p$  is the volume of the particle,  $d_p = 1.05 \text{ g/cm}^3$  is the density of the particle,  $d_w$  is the density of water,  $g = 9.8 \text{ m/s}^2$  is the acceleration due to gravity, and  $\theta = 45^\circ$ . The coefficient of viscous drag was  $\gamma = 6\pi\zeta r \approx 4 \times 10^{-8} \text{ N}\cdot\text{s/m}$ , where  $\zeta = 1$  centipoise is the viscosity of water. The Einstein relation yields  $D = k_B T/\gamma \approx 1 \times 10^{-13} \text{ m}^2/\text{s}$  for the diffusion coefficient. The amplitude  $\Delta U$  was taken to be greater than  $2 \times 10^{-16} \text{ J}$  ( $\Delta U/L > 20 \text{ pN}$ ) so that the particle has time to reach the bottom of the well while the potential is on. Such a large  $\Delta U$  is necessary for the approximations inherent in this simple picture given to be fulfilled. An exact calculation using the diffusion equation results in qualitatively the same behavior for smaller values of  $\Delta U$ . **(C)** Schematic illustration of an apparatus for separating particles with the use of biased Brownian motion combined with gravity.



### A Fluctuating Potential, or "Flashing" Ratchet

To see how thermal noise combined with an externally modulated anisotropic potential can lead to unidirectional transport, consider the model (7, 27) shown in Fig. 2A. A particle subject to viscous damping moves along a track where an anisotropic potential with periodically spaced wells at positions  $iL$  cyclically turns, or "flashes," on and off. To show that work can be done against an external force, the potential profiles are illustrated with a net force  $F_{\text{ext}}$  acting from right to left.

If the external force is not too large, the particle is pinned near the bottom of one of

the wells (for example, at  $x = 0$ ) when the potential is on. Without noise, the particle would move to the left with a velocity  $F_{\text{ext}}/\gamma$  when the potential is off, where  $\gamma$  is the coefficient of viscous drag. Thermal noise changes the situation dramatically. Because of Brownian motion, a random walk is superimposed on the deterministic drift, and the position of the particle can be determined only in terms of a probability distribution. While the potential is off, the probability distribution drifts downhill with a velocity  $F_{\text{ext}}/\gamma$  and spreads out like a Gaussian function. After a time  $t_{\text{off}}$  the distribution (Fig. 2A) is (28)

$$P(0|x;t_{\text{off}}) = \frac{\exp\left[-\frac{(x - t_{\text{off}}F_{\text{ext}}/\gamma)^2}{4Dt_{\text{off}}}\right]}{\sqrt{4\pi Dt_{\text{off}}}} \quad (1)$$

where  $D$  is the diffusion coefficient. When the potential is turned on again, the particle is trapped in the well at  $iL$  if it is between  $L(i - 1 + \alpha)$  and  $L(i + \alpha)$ . The probability of finding the particle in each well,  $P_{iL}$ , is calculated by integrating the probability density (Eq. 1) between these limits. Because of the anisotropy of the potential, a particle starting at  $iL$  is more likely to be trapped in the well at  $(i + 1)L$  than in the well at  $(i - 1)L$  for small enough  $F_{\text{ext}}$  and intermediate values of  $t_{\text{off}}$ . The average number of steps  $R$  in a cycle of turning the potential on for a time  $t_{\text{on}}$  long enough that the particle reaches the bottom of a well ( $t_{\text{on}} > \gamma L^2/\Delta U$ ), off for a time  $t_{\text{off}}$ , and then back on again, is  $R = \sum_{i=-\infty}^{\infty} i P_{iL}$ , and the average velocity is  $\langle v \rangle = RL/(t_{\text{off}} + t_{\text{on}})$  (Fig. 2B). Motion to the right occurs despite the fact that the macroscopic force pushes the particle to the left. For large  $\Delta U/L$ , the external force necessary to cause the flow to be identically zero,  $F_{\text{stop}}$  (the stopping force), can be evaluated exactly (21) to be  $F_{\text{stop}} = (\gamma L/t_{\text{off}})(\alpha - 1/2)$ . For  $t_{\text{off}} < (\gamma L/F)(\alpha - 1/2)$ , only the terms due to integration of Eq. 1 with  $i = \pm 1$  contribute to the velocity. In this regime, velocities scale with  $D/L$  and times with  $L^2/D$ .

The mechanism illustrated in Fig. 2 works not despite diffusion and thermal noise but because of diffusion. When the potential is turned off, the particle diffuses symmetrically. Then, when the anisotropic potential is turned on, it is more likely for the particle to feel a force to the right than to the left. Thus, net motion to the right occurs, even in the presence of a small homogeneous force to the left. The energy to drive the transport, however, does not come from thermal noise but is provided when the potential is turned on. This energy can be calculated by integrating over space the product of  $U_{\text{on}}(x)$  and the probability density  $P(0|x; t_{\text{off}})$ . Be-

cause the potential remains on for long enough to allow the particle to reach the bottom of a well, no energy is returned when the potential is turned off. The output energy per cycle is the number of steps  $R$  multiplied by the energy gain per step  $F_{\text{ext}}L$ . The difference in these energies is dissipated as heat resulting from viscous drag of the particle with the solvent. For the simple model shown in Fig. 2, the thermodynamic efficiency is less than 5% (29). Other features of biased Brownian motion make it more promising for the construction of microscopic motors. With a spatial period of 10  $\mu\text{m}$ , velocities of around 0.3  $\mu\text{m/s}$  can be achieved for a 2- $\mu\text{m}$  particle with  $t_{\text{off}} \approx 2$  s in aqueous solution (Fig. 2B, solid line). This motor can do work against a force as large as 0.05 pN, easily overcoming gravity, which for a 2- $\mu\text{m}$  particle with a density of 1.05  $\text{g/cm}^3$  in water is  $\approx 0.004$  pN. Larger particles, however, cannot overcome gravity and drift to the left when  $t_{\text{off}}$  is large enough (Fig. 2B, dashed line).

The velocity depends nonmonotonically on the frequency of modulation (Fig. 2B). This can be understood in terms of the competing requirements that a particle be able to diffuse at least the short distance  $\alpha L$  but not the longer distance  $(1 - \alpha)L$  while the potential is off. The nonmonotonic behavior allows for the possibility of tuning a device to a frequency characteristic to a particular particle. This tuning may be useful in applications for separating particles on the basis of size, but the bandwidth of the response is relatively broad. One can exploit this dependence, however, by imposing an external force so that some particles will move to the right and others to the left. The simplest example (Fig. 2C) is to tilt an apparatus such as that shown in Fig. 1A so that the particles experience a net gravitational force  $F_{\text{grav}}\sin(\theta)$ , where  $\theta$  is the angle relative to a horizontal surface. Small particles will feel only a small force due to gravity and a larger amount of Brownian motion, which can be biased by the ratchet to cause motion uphill to the right. The larger particles have less Brownian motion and feel a greater force due to gravity and so move downhill to the left. In such an apparatus, a mixture of particles of different sizes can be introduced in the middle, and purified fractions can be collected continuously on either end. Because of the close spacing of the electrodes, only a small voltage is necessary to achieve sufficiently large energy barriers.

The approach shown in Fig. 2C is not appropriate for smaller particles because gravity is not sufficiently strong. However, other similar strategies can be adopted, in-

cluding the use of a constant electric field as the homogeneous force (16). It has even been shown that with a more complicated pulse protocol than a simple square wave, particles of different sizes can be induced to move in opposite directions without any homogeneous long-range force at all (12, 13, 15). By exploiting the different scaling for biased Brownian motion and motion induced by deterministic gravitational and electric forces, approaches for continuous separation of particles ranging from macromolecular ( $10^{-8}$  m) to mesoscopic ( $10^{-5}$  m) size are possible.

The basic principles of motion induced by a fluctuating potential have recently been tested in simple model systems. Rouselet *et al.* (17) applied a time-dependent ratchet potential to colloidal particles using a series of interdigitated “Christmas tree” electrodes deposited on a glass slide by photolithography. Cyclically turning the potential on and off resulted in net flow. Despite the complexity of dealing with a suspension of many interacting particles, the data agreed at least semiquantitatively with the predictions of the simple theory. A similar effect was demonstrated by Faucheux *et al.* (18), who used a single colloidal particle in an optical trap modulated to generate a sawtooth potential. This setup has the advantage that there is only one particle, thus eliminating interparticle hydrodynamic interactions.

Modulating the potential certainly requires work, and there is no question of these devices being “perpetual motion machines.” The surprising aspect is that flow is induced without a macroscopic force—all of the forces involved are local and act on a length scale of the order of a single period of the potential—yet the motion persists indefinitely, for many periods. In contrast, conventional techniques for particle separation such as centrifugation, chromatography, or electrophoresis all rely on macroscopic gradients and can only operate as “batch” separators.

### A Fluctuating Force, or “Rocking” Ratchet

In the mechanism shown in Fig. 2, the spatial average of the force is independent of time, and the temporal modulation only changes the shape of the potential locally. Another well-studied approach to driving flow on a ratchet potential involves applying a fluctuating net force (6, 11, 14, 23, 30, 31). This approach can be visualized as rocking the sawtooth potential shown in Fig. 1C back and forth between the limits  $\pm F_{\text{max}}$  (Fig. 3). If  $\Delta U/[(1 - \alpha)L] < |F_{\text{max}}| < \Delta U/(\alpha L)$ , the potential energy decreases monotonically to the left when the force is

$-F_{\max}$ , but when the force is  $+F_{\max}$ , there remain minima that trap a particle as it moves to the right in response to the applied force (Fig. 3A). Thus, even without thermal noise, a slow oscillation of the force between  $\pm F_{\max}$  causes net flow to the left. Fast oscillation does not result in net flow because the particle does not have time to move a period  $L$  before the force reverses sign. Applying a fluctuating or oscillating force is analogous to the standard way of driving an electrical rectifier or a macroscopic mechanical ratchet such as a car jack or ratcheting screwdriver.

The presence of thermal noise allows a subthreshold fluctuating force  $\{|F_{\max}| < \Delta U/[(1 - \alpha)L]\}$  to cause flow (6). For a slow, zero-average square wave modulation of the force between  $\pm F_{\max}$ , the average rate can be calculated using the analytic formula given by Magnasco (6). In Fig. 3B, the average velocity is plotted as a function of  $F_{\max}$  where the dashed lines indicate the location of the threshold forces  $\Delta U/[(1 - \alpha)L]$  and  $\Delta U/(\alpha L)$ . In Fig. 3C, the average velocity is plotted as a function of the thermal noise strength  $k_B T$  (where  $k_B$  is Boltzmann's constant and  $T$  is temperature) for a subthreshold applied force ( $F_{\max} = 0.4$  pN). We see that, to a point, increasing the noise can actually increase the flow induced by the fluctuating force, which suggests that in some technological applications, it may be useful to electronically add noise to the system. For forces near the optimum ( $F_{\max} =$

1.5 pN in Fig. 3B), however, the velocity decreases almost monotonically with increasing noise.

## A More General Approach

A more general approach to investigating fluctuation-driven transport involves solving the diffusion equation

$$\frac{\partial P(x,t)}{\partial t} = -\frac{\partial}{\partial x} \left[ \frac{U'(x)}{\gamma} P(x,t) \right] + D \frac{\partial^2 P(x,t)}{\partial x^2} \quad (2)$$

At equilibrium, the probability density is given by a Boltzmann distribution  $P(x) \propto \exp(-U/k_B T)$ . Any external temporal modulation of  $U$ , whether accomplished periodically or randomly in time, requires energy input and drives the system away from equilibrium, disturbing the Boltzmann distribution. The time dependence of  $U$  for a fluctuating potential ratchet is  $U(x, t) = U_{\text{saw}}(x)$ , and for a fluctuating force ratchet, is  $U(x, t) = U_{\text{saw}}(x) + x f(t)$ . Equation 2 can be solved for  $P(x, t)$  for any explicit time dependence of  $f(t)$  with appropriate (typically periodic) boundary conditions, and the result can be used to calculate the average velocity. It turns out, however, that in many cases, it is simpler to solve Eq. 2 when  $f(t)$  is modeled as a position-independent stochastic variable (31). This situation must not be confused with an equilibrium fluctuation. At equilibrium, the probability to undergo a transition from one state to an-

other depends on the energy difference between the states according to a Boltzmann relation (also known as detailed balance), and the energy difference for a ratchet potential clearly depends on the position. An external modulation, whether random or not, does not conform to detailed balance and cannot model equilibrium fluctuations.

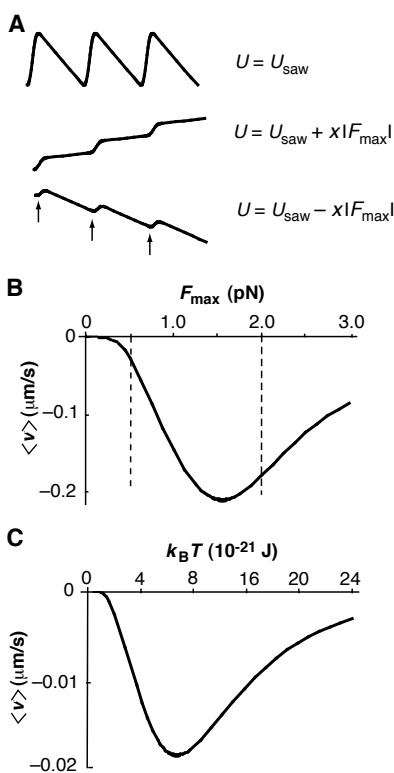
Unlike motion driven by forces such as gravity or macroscopic electric fields, where the direction of motion is determined by the sign of the force, the direction of flow induced by zero-average modulation of a potential or force depends on the details of how the modulation is carried out. Recently, several schemes have been proposed that allow for flow reversal to occur as a function of the modulation frequency, with different reversal frequencies for particles with different diffusion coefficients (13–18).

## Chemically Driven Transport

Consider the one-dimensional motion of a charged particle along a periodic lattice of dipoles arranged head to tail (Fig. 1B), and let the interaction between the particle and lattice be purely electrostatic (7). The potential energy profile then consists of a periodic series of minima (wells) and maxima (barriers). For simplicity, this profile can be represented as a sawtooth function (Fig. 1C). Because of thermal noise, the particle undergoes Brownian motion. Occasionally, it will have enough energy to pass over one of the two barriers surrounding the well in which it starts and move to the well on the right or on the left. Despite the anisotropy, without an energy supply, the two probabilities are exactly equal.

Now, imagine that this particle catalyzes a chemical reaction  $HS \rightleftharpoons H^+ + S^-$ . Because the product molecules  $H^+$  and  $S^-$  are charged, the amplitude of the interaction potential between the particle and the dipole lattice depends on whether  $H^+$  or  $S^-$  are bound to the particle, resulting in a coupling between the chemical reaction and the diffusion of the particle along the dipole lattice. Because of the charge on  $H^+$  and  $S^-$ , their local concentrations vary as a function of position along the axis of the dipole lattice (the hydrogen ion concentration  $[H^+]$  is larger near the negative end of the dipole than near the positive end, and the opposite is true for  $[S^-]$ ). The radii of the ions  $H^+$  and  $S^-$  are very small compared to the radius of the particle, so their local concentrations equilibrate quickly, leading to  $[S^-] = [S^-]_{\text{bulk}} \exp[-U(x)/k_B T]$  and  $[H^+] = [H^+]_{\text{bulk}} \exp[+U(x)/k_B T]$ , where the subscript "bulk" denotes the concentration far from the surface of the dipole lattice. For the specific mechanism shown in Fig. 4A,  $k_{21}$ ,  $k_{23}$ , and  $k_{31}$  are first-order

**Fig. 3.** The basic mechanism by which a fluctuating or oscillating force can cause directed motion along a ratchet potential  $U_{\text{saw}}$ . The parameters  $\Delta U = 4 \times 10^{-18}$  J,  $L = 10$   $\mu\text{m}$ , and  $\alpha = 0.2$  were used. **(A)** Because of the anisotropy of the potential  $U_{\text{saw}}$ , starting at the bottom of any well, the force required for the particle to move to the right,  $\sim \Delta U/(\alpha L) = 2$  pN, is greater than the force necessary to move to the left,  $\sim \Delta U/[(1 - \alpha)L] = 0.5$  pN. When an external force between these values (such as  $-1.5$  pN) is applied, the net potential  $U(x) = U_{\text{saw}} - x(-1.5$  pN) decreases monotonically to the left, and a particle acted on by this potential drifts to the left with no impediment. When an external force of  $+1.5$  pN is applied, the net potential  $U(x) = U_{\text{saw}} - x(+1.5$  pN) decreases on average to the right, but there remain wells (local potential minima, indicated by the vertical arrows) that tend to trap the particle. Thus a square wave modulation of the external force  $F_{\max}$  between  $+1.5$  pN and  $-1.5$  pN results in net flow to the left. **(B)** For a low-frequency square wave modulation, the average velocity can be calculated as a function of  $F_{\max}$  with the analytic formula given by Magnasco (6). The average velocity  $\langle v \rangle$  depends nonmonotonically on the amplitude  $F_{\max}$  and is maximum between  $F_{\max} = \Delta U/[(1 - \alpha)L] = 0.5$  pN and  $F_{\max} = \Delta U/(\alpha L) = 2$  pN (indicated by the dashed lines). Because of thermal noise, a subthreshold force  $F_{\max} < \Delta U/[(1 - \alpha)L]$  can induce some flow. **(C)** The dependence of the flow on the thermal noise amplitude  $k_B T$  induced by a 0.4-pN force. The curve is nonmonotonic, reminiscent of a phenomenon known as "stochastic resonance" (32, 33).



rate constants and do not depend on the position along the dipole, and  $k_{12} = k_{12}[\text{SH}]$ ,  $k_{13} = k_{13}[\text{H}^+]$ , and  $k_{32} = k_{32}[\text{S}^-]$  are pseudo-first-order rate coefficients into which the concentrations of the reactants have been incorporated. Because  $[\text{H}^+]$  and  $[\text{S}^-]$  depend on the position  $x$  along the dipole lattice, the rate coefficients  $k_{13}$  and  $k_{32}$  also depend on position.

If the chemical reaction is at equilibrium, a direct transition from the uncharged state  $i = 3$  to the charged state  $i = 2$  is more likely near the positive end of the dipole, where  $[\text{S}^-]$  is relatively high, than near the negative end of the dipole, where  $[\text{S}^-]$  is relatively low. Similarly, direct transition from the charged state  $i = 1$  to the uncharged state  $i = 3$  is more likely near the negative end of the dipole, where  $[\text{H}^+]$  is relatively high, than near the positive end of the dipole, where  $[\text{H}^+]$  is relatively low. The net effect is that transitions from the charged to the uncharged state are more likely near the negative end of the dipole, and transitions from the uncharged to charged state are more likely near the positive end of the dipole. In this case (and in the absence of an external force), the probability density of the particle is distributed everywhere according to a Boltzmann distribution (Fig. 4B, dashed line), and the average velocity of the particle is zero.

If the chemical reaction is away from equilibrium, this relation between the position of the particle and transition probabilities does not necessarily hold (Fig. 4B, solid line). In the extreme case where  $[\text{H}^+] = [\text{S}^-] = 0$ , direct transitions from state 1 to state 3 and from state 3 to state 2 cannot occur at all. None of the rate coefficients for the remaining transitions depend on the position of the particle, and so the probability of a transition from the charged to the uncharged state is independent of the position along the axis of the dipole lattice, as is the probability for a transition from the uncharged to the charged state. This situation is essentially identical to that described as a fluctuating potential ratchet (Fig. 2), and as before, directed motion can result.

Thus, we have a rudimentary motor driven by a chemical reaction. The mechanism shown in Fig. 4A is a tremendous oversimplification as a description of any actual molecular motor. The interaction between the motor and dipole lattice and the effect of the catalyzed reaction were assumed to be purely electrostatic, and the resulting periodic potential was grossly simplified. Nevertheless, with reasonable values of the rate constants and other parameters, the motor moves pretty well (Fig. 4C), with a maximal velocity of several micrometers per second. The stoichiometry is poor: It takes more than 3 HS molecules

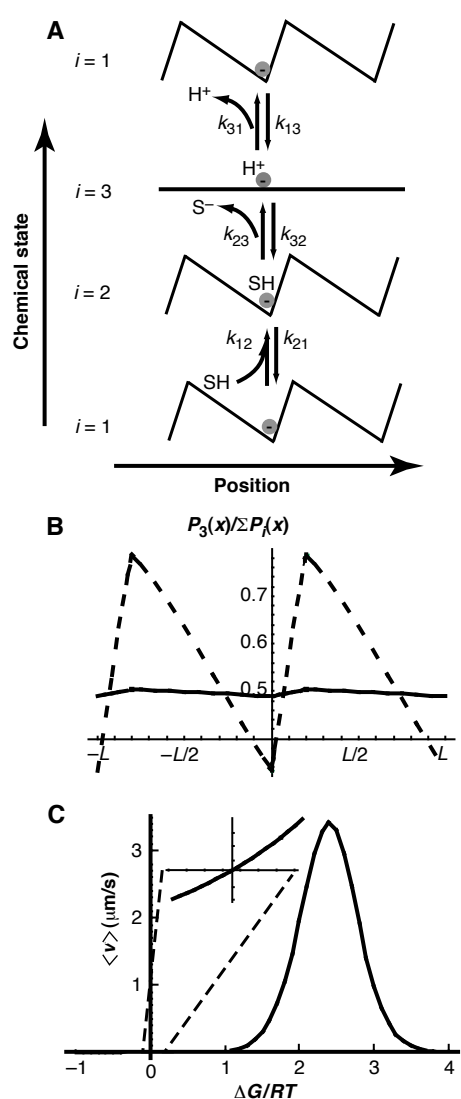
on average to cause a single step (displacement by a period  $L$ ), and less than 1 pN of applied force stops the motion. What this simplified motor lacks is what a real biomolecular motor can certainly provide: more complex interaction between the motor and track, provided by conformational flexibility, and better regulated coupling between chemical and mechanical events, possibly provided by allosteric interaction between the motor and track.

## Perspective and Outlook

Noise is unavoidable for any system in thermal contact with its surroundings. In technological devices, it is typical to incorporate mechanisms for reducing noise to an absolute minimum. An alternative approach is emerging, however, in which attempts are made to harness noise for useful purposes.

**Fig. 4.** Transport driven by a chemical reaction. **(A)** Schematic illustration of how the potential energy profile of a Brownian particle that catalyzes a reaction  $\text{SH} \rightleftharpoons \text{S}^- + \text{H}^+$  changes depending on its chemical state, even in a constant electric potential due to a dipole array as shown in Fig. 1B. **(B)** Probability of the particle being uncharged  $P_3(x)/\Sigma P_i(x)$  as a function of position when the chemical reaction  $\text{SH} \rightleftharpoons \text{S}^- + \text{H}^+$  is at equilibrium (dashed curve) and far from equilibrium (solid curve). For simplicity, we treat the case that the particle bears a charge of  $-1$  and that the interaction potential between the particle and dipole track (Fig. 1B) is purely electrostatic. Because  $\text{S}^-$  and  $\text{H}^+$  are charged, their local concentrations depend on the local potential according to  $[\text{S}^-] = [\text{S}^-]_{\text{bulk}} \exp[-U(x)/k_B T]$  and  $[\text{H}^+] = [\text{H}^+]_{\text{bulk}} \exp[+U(x)/k_B T]$ . The rate constants used were  $k_{12} = 10[\text{SH}]$ ,  $k_{21} = 10^6$ ,  $k_{23} = 10^6$ ,  $k_{32} = 10[\text{S}^-]$ ,  $k_{13} = 100[\text{H}^+]$ , and  $k_{31} = 100$ , all in inverse milliseconds, and the concentrations were  $[\text{SH}] = 4$ ,  $[\text{H}^+]_{\text{bulk}} = 2$ , and  $[\text{S}^-]_{\text{bulk}} = 2$  for the equilibrium case, and  $[\text{SH}] = 20$ ,  $[\text{H}^+]_{\text{bulk}} = 0.05$ , and  $[\text{S}^-]_{\text{bulk}} = 0.05$  for the far from equilibrium case, all in millimolar. The amplitude of the potential  $\Delta U$  was  $10^{-20}$  J. **(C)** Average velocity as a function of the  $\Delta G$  of the chemical reaction using the rate constants and field amplitude as in (B). This result can be calculated in general by using reaction-diffusion equations to describe the combined physical motion and chemical reaction of a catalytic Brownian particle as described elsewhere (9, 10). Here,  $k_{12}$  and  $k_{23}$  were taken to be large so that state 2 could be treated as a steady-state intermediate. Then, there are effectively only two states, “off” and “on,” as in Fig. 2, with the effective time constants  $\tau_{\text{off}} = \{5[\text{S}^-]_{\text{bulk}} \exp[-U(x)/k_B T] + 100\}^{-1}$  and  $\tau_{\text{on}} = \{5[\text{SH}] + 100[\text{H}^+]_{\text{bulk}} \exp[+U(x)/k_B T]\}^{-1}$ , as described in (9). The value of  $\Delta G = -RT \ln\{([\text{SH}]/([\text{S}^-]_{\text{bulk}}[\text{H}^+]_{\text{bulk}}])\}$  ( $R$  is the universal gas constant) was varied by varying  $[\text{SH}]$  with constant  $[\text{S}^-]_{\text{bulk}} = [\text{H}^+]_{\text{bulk}} = 1$ . The period  $L$  was taken to be  $10^{-8}$  m, and the viscosity at the interface was taken to be greater than in bulk water ( $\zeta_{\text{int}} = 100$  cP), resulting in  $\gamma = 6\pi\zeta r \approx 2 \times 10^{-8}$  N·s/m for a particle with a Stokes radius of  $r = 10^{-8}$  m and a diffusion coefficient  $D = 2 \times 10^{-13}$  m<sup>2</sup>/s. The inset shows that there is a linear relation between flow and  $\Delta G$  close to equilibrium. The nonmonotonic dependence on  $\Delta G$  arises because  $\Delta G$  is changed by varying the chemical concentrations, which also varies the time scales.

One example involves signal detection by threshold detectors (32). Typically, such devices have been designed so that the system is isolated from noise, and the threshold is as small as possible. These goals, however, are often difficult and expensive to attain. It may instead be possible to operate the system with a threshold larger than the signal to be measured and to use added noise to provide a boost that will allow the signal to be detected above the noise. The phenomenon of noise-enhanced signal-to-noise ratio is known as stochastic resonance and holds for a wide variety of nonlinear systems (32, 33). Similarly, fluctuation-driven transport uses noise to accomplish mass transport without macroscopic forces or gradients. Three ingredients are essential: (i) thermal noise to cause Brownian motion; (ii) anisotropy arising from the structure of the medium in which



the particle diffuses; and (iii) energy supplied either by an external variation of the constraints on the system or by a chemical reaction far from equilibrium.

It is often overlooked that noise-assisted processes incorporate features analogous to chemical kinetics (34). Transitions along a chemical pathway are described in terms of rate constants that reflect the probability that thermal noise will provide sufficient energy to surmount an energy barrier separating chemical states. Experiments on ion pumps have shown that energy from externally imposed electric oscillations (21) and fluctuations (22) can substitute for energy from hydrolysis of ATP to power uphill transport of ions. The likely mechanism involves biasing thermally activated steps in the reaction pathway—a Brownian ratchet mechanism (5, 19). As Lauger summarized, “Ion pumps do not function by a ‘power-stroke’ mechanism; instead, pump operation involves transitions between molecular states, each one of which is very close to thermal equilibrium with respect to its internal degrees of freedom, even at large overall driving force” (35).

It is not yet clear whether molecular motors such as muscle (myosin) or kinesin move by using an ATP-driven power stroke—a viscoelastic relaxation process in which the protein starts from a nonequilibrium conformation after phosphate release and which does not require thermal activation—or whether energy from hydrolysis of ATP is used to bias thermally activated steps. The recent work on Brownian ratchets shows that a thermally activated mechanism is not inconsistent with a process in which a protein moves a distance of 10 nm in a single step and generates a force of several piconewtons. This question may be resolved soon with the use of recently developed techniques for studying molecular motors at the level of a single molecule (36).

Incorporation of thermal motion as an essential element in the design of microscopic machines is essentially the equivalent of adopting design principles borrowed from chemistry rather than from classical macroscopic physics. A remarkable feature is that the fundamentally stochastic nature of noise-assisted “activated”

transitions can give rise to mechanisms that rival purely deterministic processes in the predictability of specific outcomes. This possibility has been discussed by Benet in a thermodynamic comparison of computers based on Brownian versus ballistic principles (37). Recent work shows that coupling many particles in a modulated ratchet potential gives rise to extraordinarily rich behavior and thermodynamic efficiencies up to 50% (38).

The use of noise in technological applications is still in its infancy, and it is far from clear what the future holds. Nevertheless, there is already much active research in the area of noise-enhanced magnetic sensing (39) and electromagnetic communication (40). The recent work on fluctuation-driven transport leads to optimism that similar principles can be used to design microscopic pumps and motors—machines that have typically relied on deterministic mechanisms involving springs, cogs, and levers—from stochastic elements modeled on the principles of chemical reactions and noise-assisted processes. Such devices would be consistent with the behavior of molecules, including enzymes, and could pave the way to construction of true molecular motors and pumps.

## REFERENCES AND NOTES

1. A. Einstein, *Ann. Phys.* **19**, 371 (1906).
2. P. Langevin, *Comptes Rendus* **146**, 530 (1908).
3. M. v. Smoluchowski, *Phys. Z.* **13**, 1069 (1912).
4. R. P. Feynman, R. B. Leighton, M. Sands, *The Feynman Lectures on Physics* (Addison-Wesley, Reading, MA, 1966), vol. 1, chap. 46.
5. R. D. Astumian, P. B. Chock, T. Y. Tsong, Y.-D. Chen, H. V. Westerhoff, *Proc. Natl. Acad. Sci. U.S.A.* **84**, 434 (1987).
6. M. Magnasco, *Phys. Rev. Lett.* **71**, 1477 (1993).
7. R. D. Astumian and M. Bier, *ibid.* **72**, 1766 (1994).
8. J. Prost, J. F. Chawin, L. Peliti, A. Ajdari, *ibid.*, p. 2652; C. S. Peskin, B. Ermentrout, G. Oster, in *Cell Mechanics and Cellular Engineering*, V. C. Mow et al., Eds. (Springer-Verlag, New York, 1994).
9. R. D. Astumian and M. Bier, *Biophys. J.* **70**, 689 (1996).
10. H.-X. Zhou and Y.-D. Chen, *Phys. Rev. Lett.* **77**, 194 (1996).
11. C. R. Doering, W. Horsthemke, J. Riordan, *ibid.* **72**, 2984 (1994).
12. J. F. Chawin, A. Ajdari, J. Prost, *Europhys. Lett.* **32**, 373 (1995).
13. M. Bier and R. D. Astumian, *Phys. Rev. Lett.* **76**, 4277 (1996).
14. M. Bier, *Phys. Lett. A* **72**, 12 (1996).
15. A. Mielke, *Ann. Phys. (Leipzig)* **4**, 476 (1995); *ibid.*, p. 721.
16. M. Tarlie and R. D. Astumian, in preparation.
17. J. Roussellet, L. Salome, A. Ajdari, J. Prost, *Nature* **370**, 446 (1994); see also S. Leibler, *ibid.*, p. 412.
18. L. P. Fauchoux, L. S. Bourdieu, P. D. Kaplan, A. J. Libchaber, *Phys. Rev. Lett.* **74**, 1504 (1995).
19. R. D. Astumian, P. B. Chock, T. Y. Tsong, H. V. Westerhoff, *Phys. Rev. A* **39**, 6416 (1989); R. D. Astumian and B. Robertson, *J. Chem. Phys.* **91**, 4891 (1990).
20. T. Y. Tsong and R. D. Astumian, *Bioelectrochem. Bioenerg.* **15**, 457 (1986); A. Fulinski, *Phys. Lett. A* **193**, 267 (1994).
21. D. S. Liu, R. D. Astumian, T. Y. Tsong, *J. Biol. Chem.* **265**, 7260 (1990).
22. T. D. Xie, P. Marszalek, Y. D. Chen, T. Y. Tsong, *Biophys. J.* **67**, 1247 (1994); T. D. Xie, Y. D. Chen, P. Marszalek, T. Y. Tsong, *Biophys. J.*, in press.
23. H. Risken, *The Fokker-Planck Equation* (Springer-Verlag, Berlin, 1989), chap. 11; see also P. Hanggi, P. Talkner, M. Borkovec, *Rev. Mod. Phys.* **62**, 251 (1990).
24. M. Buttiker and R. Landauer, in *Nonlinear Phenomena at Phase Transitions and Instabilities*, T. Riste, Ed. (Plenum, New York, 1982), p. 111.
25. M. Buttiker, E. P. Harris, R. Landauer, *Phys. Rev. B* **28**, 1268 (1983).
26. R. Landauer and M. Buttiker, *Phys. Scr.* **T9**, 155 (1985).
27. A. Ajdari and J. Prost, *C. R. Acad. Sci. Paris* **315**, 1635 (1992).
28. H. C. Berg, *Random Walks in Biology* (Princeton Univ. Press, Princeton, NJ, 1983).
29. M. Bier and R. D. Astumian, *Bioelectrochem. Bioenerg.* **39**, 67 (1996).
30. M. Millonas and M. M. Dyckman, *Phys. Lett. A* **185**, 65 (1994); R. Bartussek, P. Hanggi, J. G. Kissner, *Europhys. Lett.* **28**, 459 (1994); R. Bartussek, P. Reimann, P. Hanggi, *Phys. Rev. Lett.* **76**, 1166 (1996).
31. C. R. Doering, *Nuovo Cimento D* **17**, 685 (1995).
32. K. Wiesenfeld and F. Moss, *Nature* **373**, 33 (1995).
33. A. R. Bulsara and L. Gammaitoni, *Phys. Today* **49**, 39 (March 1996); R. D. Astumian, J. C. Weaver, R. K. Adair, *Proc. Natl. Acad. Sci.* **92**, 3740 (1995).
34. R. D. Astumian and B. Robertson, *J. Am. Chem. Soc.* **115**, 11063 (1993); R. D. Astumian, *J. Phys. Chem.* **100**, 19075 (1996).
35. P. Lauger, *Electrogenic Ion Pumps* (Sinauer, Sunderland, MA, 1991), p. 56.
36. J. Finer, R. M. Simmons, J. A. Spudich, *Nature* **368**, 113 (1994); K. Svoboda, C. F. Schmidt, B. J. Schnapp, S. M. Block, *ibid.* **365**, 721 (1994).
37. C. H. Bennet, *Int. J. Theor. Phys.* **21**, 905 (1982).
38. I. Derenyi and T. Vicsek, *Phys. Rev. Lett.* **75**, 374 (1995); F. Julicher and J. Prost, *ibid.*, p. 2618; I. Derenyi and A. Ajdari, *Phys. Rev. E* **54**, R5 (1996).
39. A. Hibbs et al., *J. Appl. Phys.* **77**, 2582 (1995); R. Rouse, S. Han, J. Luckens, *Appl. Phys. Lett.* **66**, 108 (1995).
40. V. S. Anishchenko, M. A. Safanova, L. O. Chua, *Int. J. Bifurcation Chaos* **4**, 441 (1994).
41. I thank B. Adair, S. Berry, C. Bagdassarian, M. Bier, I. Derenyi, G. Fried, B. Glick, D. Grier, M. Hochstrasser, S. Kron, M. Mäkinen, J. Ross, T. Steck, M. Tarlie, and T. Tsong for useful and enjoyable discussions. This work was supported in part by NIH grant R29ES06620 and the Materials Research Science and Engineering Center (MRSEC) program of the NSF (award DMR-9400379).